

Faraday Discussions

Accepted Manuscript



This manuscript will be presented and discussed at a forthcoming Faraday Discussion meeting. All delegates can contribute to the discussion which will be included in the final volume.

Register now to attend! Full details of all upcoming meetings: <http://rsc.li/fd-upcoming-meetings>



This is an *Accepted Manuscript*, which has been through the Royal Society of Chemistry peer review process and has been accepted for publication.

Accepted Manuscripts are published online shortly after acceptance, before technical editing, formatting and proof reading. Using this free service, authors can make their results available to the community, in citable form, before we publish the edited article. We will replace this *Accepted Manuscript* with the edited and formatted *Advance Article* as soon as it is available.

You can find more information about *Accepted Manuscripts* in the [Information for Authors](#).

Please note that technical editing may introduce minor changes to the text and/or graphics, which may alter content. The journal's standard [Terms & Conditions](#) and the [Ethical guidelines](#) still apply. In no event shall the Royal Society of Chemistry be held responsible for any errors or omissions in this *Accepted Manuscript* or any consequences arising from the use of any information it contains.

ARTICLE

Cite this: DOI: 10.1039/x0xx00000x

Received 00th January 2012,
Accepted 00th January 2012

DOI: 10.1039/x0xx00000x

www.rsc.org/

Solvent tuned single molecule dual emission in protic solvents: effect of polarity and H-bonding

S. Chevreux,^a C. Allain,^{*b} L. Wilbraham,^c K. Nakatani,^b P. Jacques,^d I. Ciofini,^c and G. Lemercier^{*a}

Phen-PENMe₂ has been recently proposed as a promising new molecule displaying solvent-tuned dual emission, highlighting an original and newly-described charge transfer model. The study of the photophysical behaviour of this molecule was extended to include protic solvents. Effects of polarity and hydrogen bonding lead to an even more evident dual emission associated with a large multi-emission band in some solvents like methanol, highlighting **Phen-PENMe₂** as a promising candidate for white light emission.

Introduction

Dual emission linked to intramolecular charge transfer (ICT) was demonstrated in 1959 in the 4-*N,N*-dimethylaminobenzonitrile (DMABN) compound by Lippert *et al.*¹ Since this discovery, many other systems exhibiting dual emission based on D- π -A push-pull systems (D and A being electron-donor and -acceptor, respectively) have been designed and published.²⁻⁵ However the origin of dual emission remains controversial. The most prominent theories propose a twisted ICT (TICT) model²⁻¹⁰ and a planar ICT (PICT) model.^{5,11} We previously published the discovery of a dual emission stemming from planar ICT (OPICT) and twisted locally excited (LE) states on 5-(4-dimethylaminophenylethynyl)-1,10-phenanthroline (**Phen-PENMe₂**).¹² A complete experimental and theoretical study in aprotic solvent yielded that emission originates mainly from a planar ICT with a cumulene-like structural form. In more polar solvents - such as acetone, acetonitrile and dimethylsulfoxide - a dual emission due to the stabilization of a twisted intermediate form (twist angle around 40°) enables access to the LE emission band.

In the present study, we assess the effect of protic solvents on the dual emission of **Phen-PENMe₂** (Figure 1). Such studies have been made on ICT molecules displaying pyrene,¹³ stilbene,¹⁴ 9-aminoacridine,^{15,16} and imidazole¹⁷ motifs as well as the 5-(4-dimethylamino-phenyl)-penta-2,4-dienoic acid ethyl ester DMAPPDE compound.¹⁸ In some of these cases, the contribution of a tautomerization (with an equilibrium being struck between keto-amine and enol-imine species) and an intramolecular H-bond render the problem more complex.^{15,16}

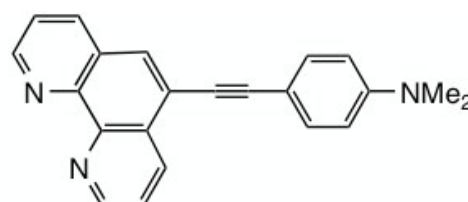


Fig. 1 Molecular structure of **Phen-PENMe₂** compound

Experimental

Materials. Methanol, ethanol, 1-propanol, 2-propanol, 1-butanol, and 1-octanol, in spectrophotometric grade, were purchased from VWR and used without further purification.

Solutions preparation. For the solvatochromism study, **Phen-PENMe₂** was dissolved in each solvent of interest to ensure that the absorbance of the final solution at 340 and 380 nm is lower than 0.1. Each solvent mixture, was prepared as desired while the final concentration of **Phen-PENMe₂** was held constant at approximately 10⁻⁵-10⁻⁶ M.

Spectroscopic measurements. UV-visible spectra were recorded on a Varian Cary 5000 and a Shimadzu UV-2401PC. Emission and excitation spectra were recorded on a Varian Cary Eclipse. The samples were conditioned in 1x1 cm quartz cuvette. Quantum yields were determined on a Fluorolog-3 equipped with an integration sphere. Quantum yields of ICT and LE were determined after irradiation at 380 and 340 nm, on deconvoluted spectra for the latter so as to discriminate ICT and LE quantum yields. The uncertainty on quantum yield measurement is estimated to be +/- 10%. CIE (Commission Internationale de l'Eclairage) coordinates were

calculated using a spreadsheet developed by Horiba Jobin Yvon and emission spectra recorded on a HJY Fluorolog-3. For the solvent mixture study, parameters (excitation and emission slit heights) were identical for all the samples. The fluorescence decay curves were obtained with the time-correlated single-photon-counting method using a Spectra-Physics titanium-sapphire Tsunami laser pumped by a Millennia Xs laser (82 MHz, repetition rate lowered to 4 MHz thanks to a pulse-picker, around 500 fs pulse width, a doubling and a tripling crystal are used to reach 330 nm excitation). Fluorescence photons were detected at 90°, through a monochromator, with a Hamamatsu MCP photomultiplier R3809U. The data were acquired using a SPC-630 TCSPC system (Becker & Hickl GmbH). The analysis was performed with the Globals software from Laboratory for Fluorescence Dynamics (LFD).

Computational details. All calculations were performed using the Gaussian 09 software.¹⁹ The basis set used for all atoms for both structural optimizations and excited states (TD-DFT) calculations was the 6-311+G(d,p). For all calculations, solvent effects of water were introduced using a conductor-like polarizable continuum model (CPCM²⁰) in addition to the explicit, site specific water molecules. Equilibrium orientation of the explicit water molecules, was determined by first placing the explicit solvent molecules close to the relevant solvation sites (NMe₂ lone pair and nitrogen atoms located on 1,10-phenanthroline) and conducting a ground state geometry optimisation. All minima on the potential energy surface were verified via the calculation of vibrational frequencies. The PBE0 functional²¹ was used throughout.

Results and discussion

Absorption spectra. UV-visible absorption spectra were recorded in various protic solvents. Changes in absorption band wavelengths are very small, indicating that the stabilization of the ground state species by the solvent is not significant (see Figure 2). In all the protic solvents used, the UV-vis absorption spectrum of **Phen-PENMe₂** is composed of (a) a broad band around 375 nm which probably corresponds to an internal charge transfer involving a flow from the donating amino group to the π^* -accepting 1,10-phenanthroline moiety (see theoretical confirmation below); the large width of this absorption band can be mainly ascribed to vibronic broadenings and/or the overlap of more bands corresponding to different close-lying electronic transitions; (b) an absorption band around 270 nm with a shoulder at lower energy, and (c) an absorption band around 220 nm which can be attributed to $n-\pi^*$ and/or $\pi-\pi^*$ transitions *a priori*.

In order to assess the character of the absorption bands, a TD-DFT investigation of the vertical absorption was conducted using water as an appropriate model for the protic solvents.

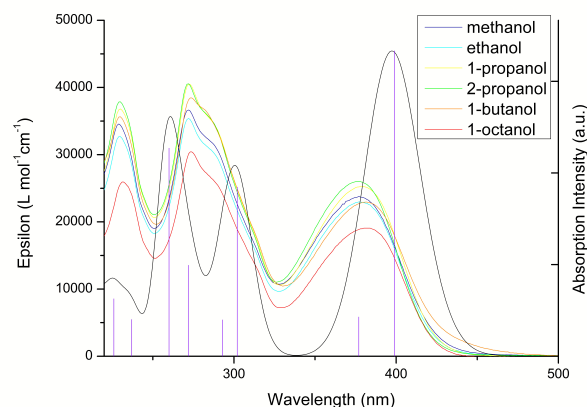


Fig. 2 Absorption spectra in epsilon in various protic solvents together with (in gray) computed spectra in water.

Bulk solvent effects were considered *via* a Polarizable Continuum Model while direct solute-solvent interactions (*i.e.* H-bond) were simulated by a minimal model of the first solvation shell, composed of only three water molecules (as depicted in Figure 3). Indeed, of these three water molecules two solvate the phenanthroline nitrogens, while the remaining water molecule solvates the amino nitrogen lone pair. These are rather strongly bounded to the **Phen-PENMe₂** molecule (computed binding energy of -14.6 kcal/mol). Details concerning the level of theory used and the model are reported in Supporting Information (see Computational Details).

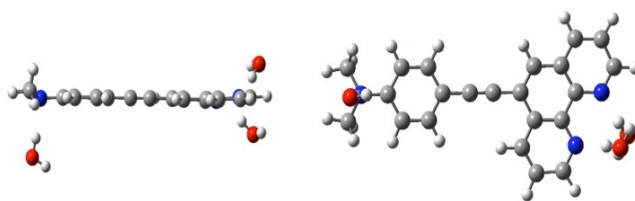
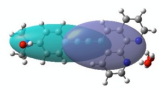
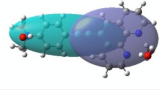
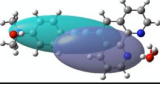
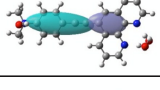
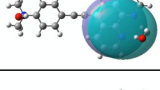
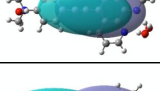
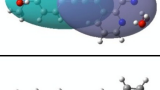


Fig. 3 Lateral and top view of the model used for calculations of **Phen-PENMe₂** in water

The computed vertical transitions as well as the simulated absorption spectrum are reported in Figure 2 together with the corresponding experimental measurements. It is clear that two main transitions (computed at 399 and 377 nm) contribute to the lowest energy band. Both transitions display a significant ICT character, inferred *via* the analysis of the Molecular Orbitals involved (reported in Supporting Information) and by the Charge Transfer distance associated with the electronic excitation (quantified by a recently developed density based index (D_{CT})²² and reported in Table 1. Indeed, a charge separation upon excitation of roughly 5.0 Å is computed for both transitions (see Table 1) corresponding to an ICT from the amino to the π^* -accepting 1,10-phenanthroline moiety. A partial - but less pronounced - ICT character is also computed for the transition predicted at 302 nm ($D_{CT} = 3.8$ Å), which clearly corresponds to the shoulder of the experimental band observed at 270 nm. Nonetheless,

all other intense transitions contributing to this band are indeed Locally Excited states (LE) corresponding to π - π^* transitions centred principally on the phenanthroline moiety.

Table 1. Computed vertical excitation energies and associated oscillator strengths (f in a.u.) together with the corresponding charge transfer distances (D_{CT}) and ellipsoids of charges. Light blue areas corresponds to density depleted zones upon excitations while gray ones corresponds to areas of increasing density upon excitation

#	Wavelength (nm)	f (a.u.)	D_{CT} (Å)	Ellipsoids of Charge
1	399	0.856	4.925	
2	377	0.110	5.168	
3	302	0.474	3.791	
5	293	0.102	5.263	
8	272	0.255	0.958	
11	260	0.583	1.713	
18	237	0.103	5.437	
22	226	0.161	3.374	

Being locally excited, these transitions are naturally accompanied by a small charge separation distance (ranging from 0.9 to 1.7 Å). Relatively strong hydrogen-bonding on both sides of the chromophore (the amino and pyridyle function(s)), may explain the *quasi* invariability of the recorded absorption characteristics between protic, and aprotic solvents (see further).

Fluorescence spectra after low energy excitation (380 nm). Emission spectra in various protic solvents were recorded after excitation at 380 nm (Figure 4). Emission displays a significant solvatochromism with a single ICT-like emission band. The band maxima range from 490 to 550 nm from the alcohol with the longest carbon chain (1-octanol) toward the shortest one (*e.g.* methanol). The observed solvatochromism is clearly smaller than reported for aprotic solvents,¹² but it is of course important to note that the Δf value range for the used protic solvents is smaller than that determined for

aprotic solvents (see Figure S1 in the Electronic Supplementary Informations, ESI).

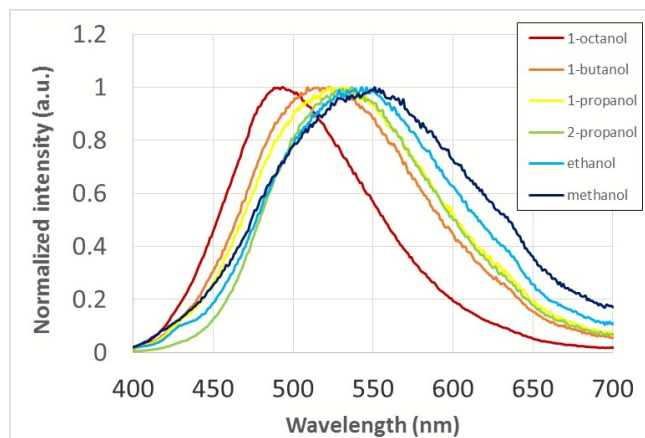


Fig. 4 Emission spectra in various protic solvent after excitation at 380 nm

Comparison between protic and aprotic solvents. In the literature, a CT band red-shift was reported in water in comparison to acetonitrile and attributed to an effect other than polarity.¹⁸ This assumption was confirmed by a red shift of the ICT band with increasing hydrogen bonding ability from 2-propanol to methanol and water.¹⁸ It was also reported that the interaction between protic solvents with the dimethyl-amino donor lead to increased stabilisation of the ground state relative to that of excited state. Stabilisation of the ground state results in a blue shift as compared to emission observed in strong polar aprotic solvents.^{14,17} In our case, the same behaviour is obtained, and the ICT band maxima in protic solvent is blue shifted comparing acetonitrile (17 762 cm^{-1}) and DMSO (17 271 cm^{-1}) to 1-butanol (19 305 cm^{-1}) and methanol (18 149 cm^{-1}), see Table S2 and S3 in the ESI.

Fluorescence spectra after higher energy excitation (340 nm). After excitation at 340 nm, the emission spectra appear very different depending on the nature of the solvent (see Figure 5).

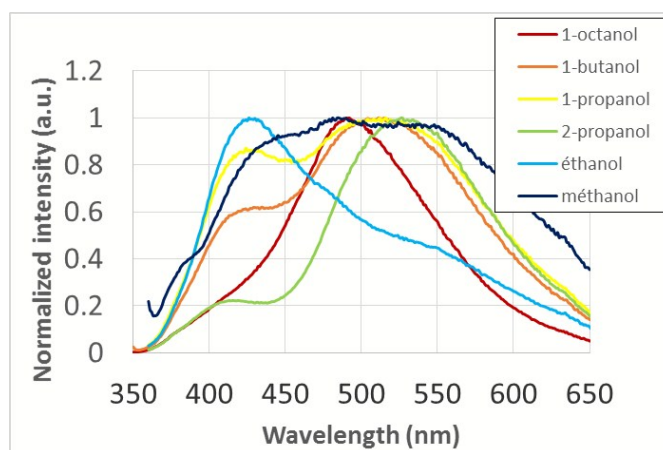


Fig. 5 Normalized emission spectra in several protic solvents after excitation at 340 nm

In 1-octanol, 1-butanol, 1-propanol, and 2-propanol the maximum wavelength of emission is located between 490 and 540 nm, and corresponds to the emission band accessible *via* lower excitation energy. A higher energy emission band is observed between 410 and 420 nm, which could be attributed to the LE emission. In ethanol, the maximum is at 425 nm with a contribution at 540 nm. This shoulder corresponds to the emission band recorded after a 380 nm excitation. The other appears after excitation at higher energy and is attributed to the LE emission. In methanol, a broader emission spectra is obtained showing several emission bands at 431, 480 and 551 nm (see Table S2 and S3 in the supplementary material). Clear separation between electronic states observed in fluorescence and in polar solvents such as alcohols has already been demonstrated (around 80 nm depending on the type of alcohol).¹⁵ In our case, the shift value is 120 nm (around 5000 cm⁻¹). This is consistent with quenching of the ICT emission by the hydrogen bonding of the lone pair on the amino moiety, opening a new fluorescence deactivation pathway. In 2-propanol for example (polar solvent with reduced ability to form hydrogen bonds), the conjugation of the system allows the ICT. On the contrary, in methanol and ethanol, LE could easily be accessible. To support this assumption, it has been shown that ICT emission is quenched by water addition to polar protic (2-propanol, methanol, ethanol, and butanol),¹⁵ and aprotic¹² solvents. To conclude, we notice that LE is dominant at higher excitation energy and ICT at lower excitation energy. Although recently observed on another type of compound (composed of 4,5-diphenyl-1H-imidazole moiety as a donor with cyanoacetic acid or 4-nitrophenyl acetonitrile as the acceptor),¹⁷ this phenomenon, specifically where generally LE is privileged and ICT is only accessible after higher energy excitation, is rare in the literature.

Excitation spectra. Comparing in 2-propanol for example, the position of absorption, emission and excitation bands of **Phen-PENMe₂** (Figure 6), it was noticed that the main emission band stems from the absorption band centred at 380 nm.

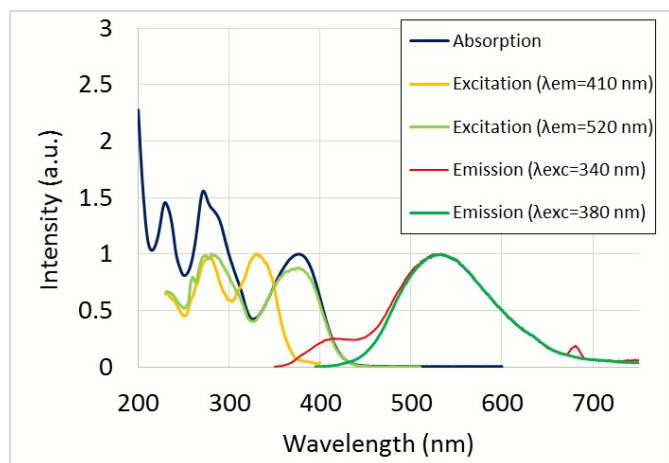


Fig. 6 Absorption, emission and excitation spectra of **Phen-PENMe₂** in 2-propanol

The highest energy emission band ($\lambda_{em} = 410$ nm) revealed after excitation at 340 nm originates from a band centred at 330 nm that is

not present on the absorption spectra. Gehlen *et al.*¹⁵ already reported such a difference between the excitation spectrum of the ICT emission band compared with its absorption spectrum in 2-propanol. The difference was claimed to be linked to the ICT band whereas, in our case, it is linked to the LE emission, as already highlighted in acetonitrile.¹²

Contrary to previous study¹⁷ and concerning the ICT emission, the two lines of the Stokes shifts correlations with Δf , for aprotic and protic solvents, are basically merging (see Fig. S1 in the ESI). Thus, the overall effect of specific interactions in protic solvents is weak, likely due to the complex interplay between the specific interactions, occurring at the three N atoms (see theoretical section). It is surprisingly observed for both the ICT, and the LE bands – even if the number of experimental points is limited for the LE in protic solvents. This is confirmed by the discontinuity observed in the $\Delta\nu_{ST}$ against $E_T(30)$ parameter (which intrinsically takes into account the H-bonding character of the solvents) representation (see Figure S2 in the ESI); the effect of H-bond should lead to a continuum in this representation. As supported by the ground state data and theoretical results reported above, this may be partially attributed to the participation of both the lone pair of the donor amino-type group, and the 1,10-phenanthroline moiety in hydrogen bond(s), with protic solvent molecule. It is also worth nothing that the LE band – which originates from hydrogen bonding in protic solvent and is further enhanced by adding water to polar solvents (such as DMSO or acetonitrile) – seems to have a different slope than the ICT.

Effect of solvent mixtures on fluorescence spectra. Emission spectra of **Phen-PENMe₂** in mixtures of various proportions of ethanol and 2-propanol were recorded after excitation at 340 nm (Figure 7).

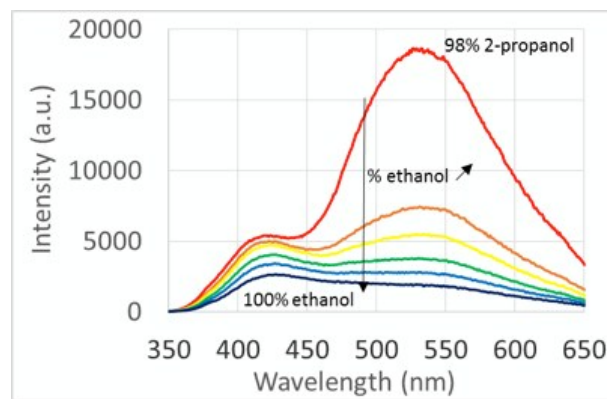


Fig. 7 Emission spectra in various mixtures of ethanol and 2-propanol after excitation at 340 nm

Due to the dependence of the quantum yield of **Phen-PENMe₂** on the solvent (Table 2), emission intensities were normalized using the area of the emission spectra (Figure 8). An *iso-emissive* point can be seen, highlighting the existence of two emissive states in different proportions according to the nature of the medium. In 2-propanol, ICT is favoured whereas in ethanol, hydrogen bonding enhances other deactivation pathways and disfavours ICT emission compared to that of the LE state.

Solvent	Φ (LE, excitation at 340 nm) %	Φ (ICT, excitation at 340 nm) %	Φ (ICT, excitation at 380 nm) %
Ethanol	1.0	0.5	0.5
2-propanol/ethanol (60/40)	1.1	5.4	7.5
2-propanol	1.5	29.4	31.2

Table 2 Quantum yield of **Phen-PENMe₂** in ethanol, 2-propanol and a mixture of these two solvents

Literature reports the existence of isosbestic and *iso*-emissive points in several mixtures of protic solvents (2-propanol and addition of methanol or water for example).¹⁶

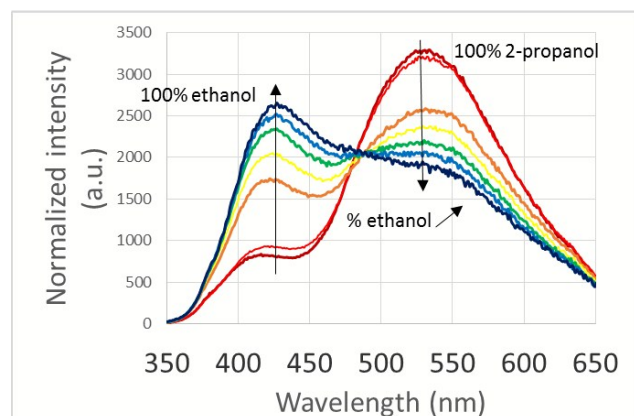


Fig. 8 Normalized emission spectra in various mixtures of ethanol and 2-propanol solvents after excitation at 340 nm.

As a consequence, the colour emission of **Phen-PENMe₂** can be tuned by changing the *ratio* of ethanol and 2-propanol solvents (figure 9) and an off-white emission ($x = 0.275$, $y = 0.330$) is observed in a mixture 2/1 of ethanol/2-propanol.

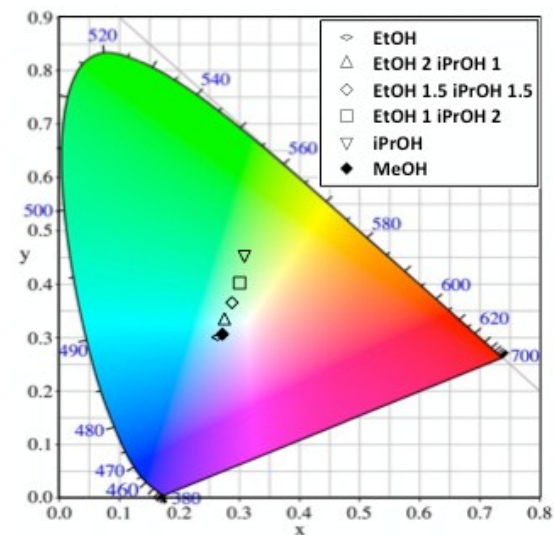


Fig. 9 CIE coordinates of **Phen-PENMe₂** in various mixtures of ethanol and 2-propanol solvents after excitation at 340 nm

When the amount of 2-propanol in the mixture of solvents increases, the intensity of the ICT band increases and the fluorescence emission takes a green colour. In our case, the dual emission phenomena can be explained by the existence of specific solute-solvent interactions; when methanol is added, a solvent hydrogen-bond with the amino function may occur and open an efficient fluorescence deactivation pathway, inhibiting the extent of conjugation. It has also been reported previously that the presence of a non-structured spectrum in glycerol at 0°C, was due to hydrogen bonding and an efficient ICT.¹³

Fluorescence quantum yield is usually higher in polar protic solvents relative to aprotic solvents: increased water solubility gives rise to reduced quantum yield.¹⁴ This is clearly shown in this work for 2-propanol but not for ethanol (smaller quantum yield compared to that in acetonitrile and DMSO). This can be explained by an overall lowering in quantum yield in solvents with greater hydrogen bonding capability attributed mainly to more efficient, non-radiative decay pathways *via* hydrogen bonding interactions between the fluorophore and protic solvents.^{17,18}

In order to complete the photophysical characterizations, fluorescence lifetimes (τ) were inspected in different mixtures of ethanol and 2-propanol solvents (Table 3). Multi-exponential components were necessary to fit correctly lifetime decays. For each exponential function, the 'A' factor corresponds to the amplitude and τ to the associated lifetime. At 330 nm, some negative contribution can be observed with increasing 2-propanol concentration by observing the ICT emission band, which is in good agreement with a transfer between LE and ICT state. LE lifetime remains unchanged between solvents (around 1.25 ns) while ICT lifetime rises one order of magnitude from ethanol to 2-propanol (from 0.2 to 2.5 ns).

Solvent	Excitation at 380 nm, emission at 540 nm		Excitation at 330 nm, emission at 600 nm		Excitation at 330 nm, emission at 410 nm	
	A	τ (ns)	A	τ (ns)	A	τ (ns)
Ethanol	0.591	0.69	0.511	1.35	7.86	1.24
	38.7	0.21	36.69	0.22	25.1	0.005
2-propanol/ethanol (60/40)	14.98	0.79	27.15	0.79	2.97	1.88
	10.94	0.06	0.191	3.22	3.18	1.25
2-propanol/ethanol (95/5)	-	-	-12.44	0.01	10.97	0.005
	6.76	2.5	11.15	2.48	2.79	1.94
	2.76	0.10	-5.2	0.03	1.62	1.25
	-	-	-	-	17	0.007

Table 3 Lifetimes and related amplitude of **Phen-PENMe₂** in mixtures of ethanol and 2-propanol

This could be explained by the higher propensity of ethanol to partake in hydrogen-bonding compared to 2-propanol, opening distinct deactivation pathway and reducing stability and emissivity of the ICT related excited state. Radiative, and non-radiative deactivation constants (k_r and k_{nr} , respectively) were also calculated for ICT and LE bands (Table 4). We notice that k_r and k_{nr} for LE remains unchanged between solvents, while k_r increases, and k_{nr} decreases by one order of magnitude from ethanol to 2-propanol. The increased non radiative de-excitation in ethanol compared to 2-propanol supports the involvement of H-bonds in secondary de-

excitation pathways. This point is illustrated by the k_r/k_{nr} values, which increase from ethanol to 2-propanol for the ICT. It is of note that this value is a constant for the LE transition in agreement with its more localized character, and is less influenced by the nature of the media.

Solvent	Emission	k_r (10^7 s $^{-1}$)	k_{nr} (10^7 s $^{-1}$)	k_r/k_{nr}
Ethanol	LE	0.8	79	0.01
	ICT	2.3	452	0.01
	ICT*	4.8	471	0.01
2-propanol/ ethanol (60/40)	LE	0.9	79	0.01
	ICT	6.8	119	0.06
	ICT*	9.5	116	0.08
2-propanol/ ethanol (95/5)	LE	1.2	79	0.02
	ICT	11.9	29	0.41
	ICT*	12.5	28	0.45

Table 4 Radiative and non-radiative deactivation constants of **Phen-PENMe₂** in mixtures of ethanol and 2-propanol after excitation at 330 nm (*excitation wavelength 380 nm)

Conclusions

To conclude, **Phen-PENMe₂**, was successfully designed, displaying original photophysical properties. As previously described in the case of aprotic solvents, dual emission arises in this study, from an ICT state and a LE state. The ICT state is accessible at low excitation energy (380 nm) while the LE state only appears at higher excitation energy (330-340 nm). In this study, steady-state and time-resolved spectroscopy illustrate that LE emission can be mainly favoured by intermolecular H bonding between the *N*-amino lone pair and protic solvents, giving rise to another deactivation pathway. Theoretical calculations on the excited-state, and transient absorption spectroscopy will be necessary to get more insight into the kinetic characteristics of this supra-molecular edifice (**Phen-PENMe₂** and surrounding protic solvent molecules); more than the steady-state study, these kinetic parameters will undoubtedly lead to information on the conditions which favour LE and/or ICT emissive excited state and explain the similarity of the UV-vis absorption spectra in protic and aprotic solvents. The exceptional luminescence properties of **Phen-PENMe₂** is of great interest for fundamental studies on dual emission and are promising for applications in the fields of optics - such as optical probes in biology - and material sciences - as sensors, and materials capable of white light emission. Finally, interesting nonlinear optical properties can be anticipated for **Phen-PENMe₂** and its use as a ligand for metal ions is currently under analysis

Acknowledgements

S.C. and G.L. thank Ms. M. Bruhammer for help with some photophysical measurements during her internship. C.A. thanks A. Brosseau for help with the lifetimes measurements and Dr. R. Métivier for kindly providing a template for Figure 9.

Notes and references

^a Reims Champagne-Ardenne University, ICMR UMR CNRS n°7312 BP 1039 – 51687 Reims cedex 2, France.

E-mail: gilles.lemercier@univ-reims.fr

^b PPSM, CNRS UMR 8531, ‡Ecole Normale Supérieure de Cachan, PPSM, 61 avenue du Président Wilson, 94235 Cachan cedex, France.

E-mail: callain@ens-cachan.fr

^c PSL Research University, Chimie ParisTech — CNRS UMR 8247, Institut de Recherche de Chimie Paris, 75005, Paris, France.

^d Université de Haute-Alsace, UHA, LPIM, EA 4567, Mulhouse, France.^d

† Footnotes should appear here. These might include comments relevant to but not central to the matter under discussion, limited experimental and spectral data, and crystallographic data.

Electronic Supplementary Information (ESI) available: [details of any supplementary information available should be included here]. See DOI: 10.1039/b000000x/

1 E. Lippert, W. Lüder and H. Boos, (*Proc. of the 4th International Meeting on Molecular Spectroscopy*, Bologna, Italy, 1959) *Advances in Molecular Spectroscopy*, ed. Mangini, A. Pergamon Press, Oxford, 1962, 443.

2 J. Catalan, *Phys. Chem. Chem. Phys.*, 2013, **15**, 8811

3 J. Catalan, *Phys. Chem. Chem. Phys.*, 2013, **15**, 16978

4 J. Catalan, *Phys. Chem. Chem. Phys.*, 2014, **16**, 7734.

5 K. A. Zachariasse, *Phys. Chem. Chem. Phys.*, 2013, **15**, 16976

6 Z. R. Grabowski, K. Rotkiewicz, W. Rettig, *Chem. Rev.*, 2003, **103**, 3899.

7 J. M. Rhinehart, R. D. Mehlenbacher and D. W. McCamant, *J. Phys. Chem. B*, 2012, **161**, 10522.

8 A. Pugliucci, E. Vauthey and W. Rettig, *Chem Phys Lett.* 2009, **469**, 115.

9 I. Gomez, Y. Mercier, M. Reguerro, *J. Phys. Chem. A*, 2006, **110**, 11455.

10 C. Cao, X. Liu, Q. Qiao, M. Zhao, W. Yin, D. Mao, H. Zhanh and Z. Xu, *Chem. Comm.* 2014, **50**, 15811.

11 K. A. Zachariasse, S. I. Druzhinin, W. Bosch and R. Machinek, *J. Am. Chem. Soc.* 2004, **126**, 1705.

12 S. Chevreux, R. Paulino Neto, C. Allain, K. Nakatani, P. Jacques, I. Ciofini and G. Lemercier, *Phys. Chem. Chem. Phys.*, 2015, **17**, 7639.

13 U. Subudhi, S. Haldar, S. Sankararaman and A.K. Mishra, *Photochem. Photobiol. Sci.*, 2006, **5**, 459.

14 C. Huang, X. Peng, D. Yi, J. Qu and H. Niu, *Sensors and Actuators B*, 2013, **182**, 521.

15 R.V. Pereira, A.P. Garcia Ferreira and M.H. Gehlen, *J. Phys. Chem. A*, 2005, **109**, 5978.

16 R. V. Pereira and M. H. Gehlen, *J. Phys. Chem. A*, 2006, **110**, 7539.

17 N. Nagarajan, G. Velmurugan, P. Venuvanalingam and R. Renganathan, *J. Photochem Photobiol A: Chemistry*, 2014, **284**, 36.

18 S. Jana, S. Dalapati, S. Ghosh and N. Guchhait, *J. Photochem. Photobiol. A: Chemistry*, 2013, **261**, 31.

19 Gaussian 09, Revision A.02, Frisch, M. J.; Trucks, G. W.; Schlegel, H. B.; Scuseria, G. E.; Robb, M. A.; Cheeseman, J. R.; Scalmani, G.; Barone, V.; Mennucci, B.; Petersson, G. A.; Nakatsuji, H.; Caricato, M.; Li, X.; Hratchian, H. P.; Izmaylov, A. F.; Bloino, J.; Zheng, G.; Sonnenberg, J. L.; Hada, M.; Ehara, M.; Toyota, K.; Fukuda, R.; Hasegawa, J.; Ishida, M.; Nakajima, T.; Honda, Y.; Kitao, O.; Nakai, H.; Vreven, T.; Montgomery, J. A., Jr.; Peralta, J. E.; Ogliaro, F.; Bearpark,

M.; Heyd, J. J.; Brothers, E.; Kudin, K. N.; Staroverov, V. N.; Kobayashi, R.; Normand, J.; Raghavachari, K.; Rendell, A.; Burant, J. C.; Iyengar, S. S.; Tomasi, J.; Cossi, M.; Rega, N.; Millam, N. J.; Klene, M.; Knox, J. E.; Cross, J. B.; Bakken, V.; Adamo, C.; Jaramillo, J.; Gomperts, R.; Stratmann, R. E.; Yazyev, O.; Austin, A. J.; Cammi, R.; Pomelli, C.; Ochterski, J. W.; Martin, R. L.; Morokuma, K.; Zakrzewski, V. G.; Voth, G. A.; Salvador, P.; Dannenberg, J. J.; Dapprich, S.; Daniels, A. D.; Farkas, Ö.; Foresman, J. B.; Ortiz, J. V.; Cioslowski, J. and Fox, D. J. Gaussian, Inc., Wallingford CT, 2009.

20 S. Miertuš, E. Scrocco and J. Tomasi, *Chem. Phys.* 1981, **55**, 117.

21 C. Adamo and V. Barone, *J. Chem. Phys.* 1999, **110**, 6158.

22 T. Le Bahers, C. Adamo, I. Ciofini *J. Chem. Theory Comput.* 2011, **7**, 2498.